Thermodynamic origin of cooperativity in actomyosin interactions: The coupling of short-range interactions with actin bending stiffness in an Ising-like model

Adriano M. Alencar
Department of Environmental Health, Harvard School of Public Health, Boston, Massachusetts 02115, USA and Department of Pathology, Medical School of the University of São Paulo, 01246–903 São Paulo, São Paulo, Brazil

James P. Butler
Department of Environmental Health, Harvard School of Public Health, Boston, Massachusetts 02115, USA and Department of Medicine, Harvard Medical School, Boston, Massachusetts 02115, USA

Srboljub M. Mijailovich
Department of Environmental Health, Harvard School of Public Health, Boston, Massachusetts 02115, USA

(Received 16 July 2008; revised manuscript received 16 February 2009; published 7 April 2009)

We present Monte Carlo simulations for a molecular motor system found in virtually all eukaryotic cells, the acto-myosin motor system, composed of a group of organic macromolecules. Cell motors were mapped to an Ising-like model, where the interaction field is transmitted through a tropomyosin polymer chain. The presence of Ca^{2+} induces tropomyosin to block or unblock binding sites of the myosin motor leading to its activation or deactivation. We used the Metropolis algorithm to find the transient and the equilibrium states of the acto-myosin system composed of solvent, actin, tropomyosin, troponin, Ca^{2+}, and myosin-S1 at a given temperature, including the spatial configuration of tropomyosin on the actin filament surface. Our model describes the short- and long-range cooperativity during actin-myosin binding which emerges from the bending stiffness of the tropomyosin complex. We found all transition rates between the states only using the interaction energy of the constituents. The agreement between our model and experimental data also supports the recent theory of flexible tropomyosin.

DOI: 10.1103/PhysRevE.79.041906 PACS number(s): 82.39.Rt, 64.60.De, 64.70.qd, 87.10.Rt

I. INTRODUCTION

Muscles are made of highly specialized cells with the ability to transform chemical free energy into force, and hence motion. This occurs in the molecular motor comprising the actin-myosin complex, where the actin fiber (F-actin) functions as a track on which a population of myosin subfragments 1 (S1) can bind and generate contraction. Using ATP hydrolysis as fuel, S1 can bind to and unbind from discrete binding sites on F-actin, within the potential wells formed between S1 and monomers of F-actin. The S1 binding dynamic is regulated by two other polymers, tropomyosin (Tm) and troponin (Tn).

Each tropomyosin covers about seven monomers on the F-actin helical strand, sterically blocking S1 motion. Troponin consists of three components: Troponin T, Troponin C, and Troponin I, denoted as TnT, TnC, and TnI, respectively. One end of TnT is bound to a specific site on Tm and its N-terminus overlaps the adjacent Tm. In the absence of calcium, the N-terminal region of TnC is closed, and the C-terminal of adjacent TnI is bound to actin, prohibiting Tm movement. Thus in relaxed muscle, TnI holds Tm in an azimuthal position $\phi^{\Downarrow}$ that sterically blocks S1 binding sites on F-actin. By contrast, during muscle activation, the presence of Ca^{2+} activates the Tn·Tm complex when Ca^{2+} binds to TnC, generating a conformational change in TnI. This conformational change alters the affinity of TnI to F-actin, releasing the TnI C terminus from F-actin, so the myosin binding site on F-actin is then exclusively regulated by tropomyosin [1,2]. After Ca^{2+} binding to TnC, the unconstrained tropomyosin moves toward an azimuthal position $\phi^{\varnothing}$, favoring actin-myosin interaction and, therefore, muscle contraction [3,4].

On the other hand, when the myosin motor head S1 binds to F-actin, it displaces the Tm·Tn complex even more, generating an angular displacement $\phi^{\Uparrow}$, which facilitates nearby S1 binding; this is a potential origin of cooperativity in binding. A schematic drawing of these geometric features is shown in Fig. 1. While the relationship between muscle contraction and the presence or absence of Ca^{2+} has been well established [5–10], the origin of S1 binding cooperativity is still in debate [11,12].

From this standpoint, we have proposed a Monte Carlo (MC) model for regulation of S1 binding, where, following the approach of Smith *et al.* [3,11,13], Tm is treated as a continuous flexible chain excited by thermally driven distortions. Our statistical mechanical model offers a way to evaluate cooperativity and a theoretical framework to describe experimental data.

II. ISING-LIKE MODEL

Although each Tm can cover only seven monomers of F-actin, the head of one Tm can connect to the tail of another forming a chain covering actin monomers along a single strand of the whole F-actin filament [14]. Hence, we consider the set of connected neighboring Tms as a single semiflexible polymer chain of length L spanning the whole F-actin strand. Assuming that the Tm chain is continuous, inextensible, and one dimensional with a nonzero bending modulus,

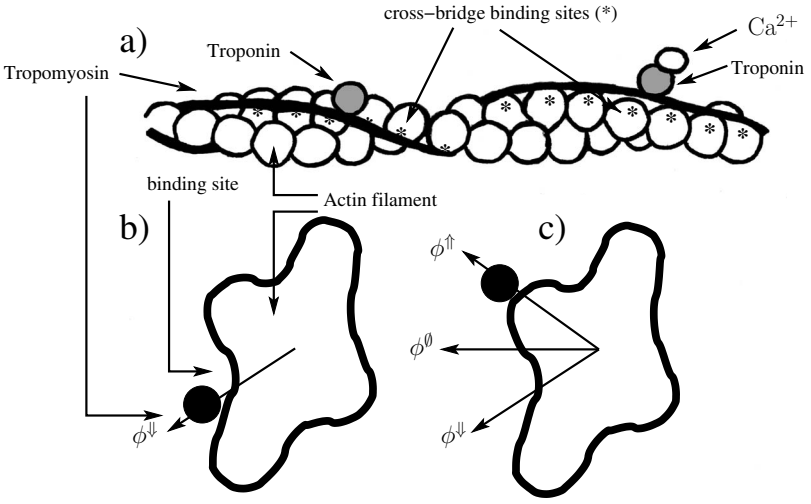

FIG. 1. Illustration of the attachment between the tropomyosin-troponin complex to actin filament highlighting the cross-bridge binding sites in two situations: on the left side of (a), there is no calcium bound to troponin and tropomyosin blocks the cross-bridge binding sites. A cross section of this configuration is depicted in (b). On the right side of (a), there is a region where calcium is bound to troponin and tropomyosin is shifted, leaving the cross-bridge sites open, i.e., accessible to myosin binding. A cross section of this configuration is depicted in (c). The angular positions of blocked, closed, and open positions are denoted as $\phi^{\Downarrow}$, $\phi^{\varnothing}$, and $\phi^{\Uparrow}$, respectively.

the potential energy E is a function of its angular displacement $\phi(s)$, where s is the arc length along the chain. Following Smith [13], we take the energy to be dominated by two terms: the first is associated with bending stiffness of the continuous flexible Tm chain and the second is associated with a quadratic potential mimicking the interaction of Tm with F-actin. The potential energy functional E can be written as

$$E = \int_0^L \left[\frac{\kappa}{2}\phi''(s)^2 + \frac{\alpha}{2}\phi(s)^2 \right] ds, \tag{1}$$

where κ is the angular bending stiffness given by the product of the chain bending stiffness and R^2, where R is the radius of actin filament upon which Tm weakly interacts with the actin surface. The strength of the confining potential [13] is given by α, which is equivalent to an angular spring constant per unit length given by the product of the usual spring constant and R^2. Here primes denote differentiation with respect to the arc length s.

When S1 binds to F-actin we call this "spin up" ($\Uparrow$), and when TnC is not activated by Ca^{2+}, i.e., when TnI holds tropomyosin pinned to actin, we call this "spin down" ($\Downarrow$). The S1 binding sites on F-actin are located on each actin monomer along each F-actin filament, thus spins up are possible at any of these sites. In contrast, following structural topology, the Tn is associated with every seventh actin site, and thus spins down are possible only at these locations, i.e., at every seventh actin monomer along an F-actin filament. We define a sequence of regions or intervals labeled I_m between any two nearest-neighbor spins; we denote the arc length of the chain segment I_m by ℓ_m. Here, the two spins define fixed points of the flexible chain segment and constitute its configuration. The energy of the chain over its full length, $L=\Sigma_m \ell_m$, can be written as a sum over energies of these segments,

$$E = \sum_m \ell_m E_m, \tag{2}$$

where E_m is the mean potential energy per unit length in the mth segment:

$$E_m = \frac{1}{\ell_m}\int_{s\in I_m} \left[\frac{\kappa}{2}\phi''(s)^2 + \frac{\alpha}{2}\phi(s)^2 \right] ds. \tag{3}$$

Note that the integral is taken inside the region I_m.

Depending on the nature of the nearest-neighbor spins, each of the regions m can be in a symmetric configuration if both spins are $\Uparrow$ or if both are $\Downarrow$, or in an asymmetric configuration if one spin is $\Uparrow$ and the other is $\Downarrow$. Using a path-integral formulation, the energy of the symmetrical configurations $E_{\Uparrow\Uparrow}$ and $E_{\Downarrow\Downarrow}$, and the asymmetrical configuration $E_{\Uparrow\Downarrow}$, has been solved [3,11];

$$E_{\Uparrow\Uparrow} = A\Gamma_s, \quad E_{\Downarrow\Downarrow} = B\Gamma_s, \tag{4}$$

$$E_{\Uparrow\Downarrow} = \frac{1}{4}[(\sqrt{A}-\sqrt{B})^2\Gamma_s + (\sqrt{A}+\sqrt{B})^2\Gamma_a], \tag{5}$$

where

$$A = 4\kappa\xi^3(\phi^{\Uparrow})^2, \quad B = 4\kappa\xi^3(\phi^{\Downarrow})^2, \quad \xi = (\alpha/4\kappa)^{1/4}, \tag{6}$$

$$\Gamma_s = N_s/D, \quad \Gamma_a = N_a/D, \tag{7}$$

where A and B are single shifts in energy, for spin-up "$\Uparrow$" and spin-down "$\Downarrow$," respectively, caused by chain displacement; $1/\xi$ is the persistence length of the tropomyosin filament; Γ_s and Γ_a are the energies of the chain in the symmetric and antisymmetric configurations, respectively, as functions of the distance between two nearest-neighbor spins. The explicit formulae for N_s, N_a, and D as functions of configuration and distance of neighboring spins used in our simulations can be found in Smith [13].

Next, we introduce an Ising-like model to solve the dynamics of this system, where spins are associated with S1 and Ca^{2+} binding activity. In this model the long-range cooperativity and correlations are transmitted through the bending stiffness of the Tm·Tn complex coupled with the short-range interaction potential between nearest neighbors.

A spin can only be at discrete actin binding sites. The distance between these sites is denoted δ. The total number of sites on one strand of F-actin is $n=L/\delta$; we fractionate the sites into $n^{\Uparrow}$ with spin up, $n^{\Downarrow}$ with spin down, and $n^{\varnothing}$ free (unoccupied) actin sites. Thus, $n=n^{\Uparrow}+n^{\Downarrow}+n^{\varnothing}$. For each site

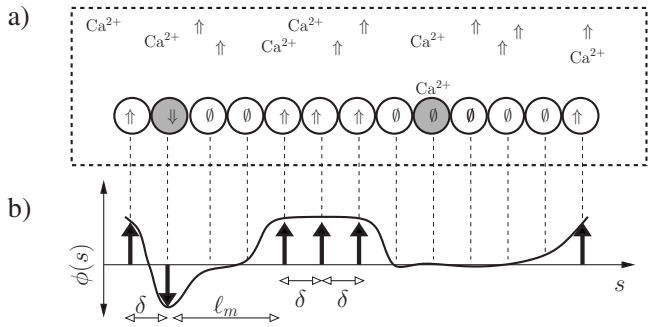

FIG. 2. The model: (a) free Ca^{2+}, spins-up "⇑," and spins-down "⇓," representing S1 and Tn, respectively, and circles representing F-actin monomers. Filled gray circles are the only sites to which Tn can bind, while S1 can bind to any actin monomer on the thin filament except the sites where troponin is bound (denoted as "⇓"); S1 in solutions (gray arrows) will form spins up upon binding to actin. Due to structural constraints the filled gray sites are located at every seventh monomer of F-actin. (b) The flexible Tm chain model with the respective spin configuration from (a). Tm chain connects all sites between the spins.

S_i along F-actin, the states $S_i = \Uparrow, \Downarrow$, and $\varnothing$ are denoted as the sites where S1 is bound to F-actin ($\Uparrow$), where TnI holds tropomyosin pinned to actin ($\Downarrow$), or where neither S1 nor TnI is bound ($\varnothing$), respectively. Hence, the state of the whole chain can be represented as a vector $\mathcal{F}=(S_1, S_2, \ldots, S_n)$ (see Fig. 2). In our model we distinguish two types of elements, active elements which can interact (S1, Tn, and Ca^{+2}) and passive elements (Tm and F-actin). The transitions of the active elements are organized as the following: (i) F-actin·Tm+Tn⇔F-actin·Tm·Tn. Tn binding to Tm in the absence of Ca^{+2} involves a chemical reaction that reduces the energy of the system to self-energy $E^{\Downarrow}$ and changes the local angular displacement of Tm from $\phi^{\varnothing}$ to $\phi^{\Downarrow}$; (ii) F-actin·Tm·Tn+Ca^{2+}⇔F-actin·Tm·Tn·Ca. Ca^{+2} activation of Tm·Tn increases the energy of the system to self-energy $E^{\varnothing}$ and changes the local angular displacement of Tm from $\phi^{\Downarrow}$ to $\phi^{\varnothing}$; (iii) F-actin+S1⇔F-actin·S1. S1 binding to an F-actin monomer reduces the energy of the system to self-energy $E^{\Uparrow}$ and changes the angular displacement of Tm from $\phi^{\varnothing}$ to $\phi^{\Uparrow}$. Note that both $E^{\Uparrow}$ and $E^{\Downarrow}$ are less than $E^{\varnothing}$.

The potential energy of the system associated with these transitions is also changed due to the Tm displacement [Eq. (1)]. The total energy can be calculated from discretized chain positions. The discrete system consists of $n^{\Uparrow}+n^{\Downarrow}-1$ segments per F-actin strand, each bounded by a pair of nearest-neighbor spins. The corresponding Hamiltonian over all segments can be written as

$$\mathcal{H}_F = n^{\Uparrow}E^{\Uparrow} + n^{\Downarrow}E^{\Downarrow} + n^{\varnothing}E^{\varnothing} + \sum_{m=1}^{n^{\Uparrow}+n^{\Downarrow}-1} E_{p(m)}, \tag{8}$$

where the sum runs over all pairs of neighboring spins; $E_{p(m)}$ is the chain energy from Eqs. (4) and (5), and $p(m)$ denotes the type of the nearest-neighbor spins, which can be "⇑⇑" or "⇓⇓" for a symmetrical, or "⇑⇓" for an asymmetrical configuration.

The number of particles of each type and the temperature of the system are assumed to be constant, and thus form a canonical ensemble, in which the expectation of any observable $A(\mathcal{F})$ is given by

$$\langle A \rangle_T = \frac{1}{Z}\int A(\mathcal{F}) e^{-\mathcal{H}\beta} d\mathcal{F}, \tag{9}$$

where $\beta = 1/k_B T$, k_B is the Boltzmann constant, and Z is the partition function of this system given by

$$Z = \int e^{-\mathcal{H}\beta} d\mathcal{F}. \tag{10}$$

The integrals in Eq. (9) and (10) represent discrete sums over all possible configurations of the system.

Our system is energetically conservative and all elements, active and passive, interact using the Metropolis algorithm on the Hamiltonian in Eq. (8). The interactions between F-actin (sites), tropomyosin (Tm), troponin (Tn), Ca^{2+}, and S1 are included in the canonical ensemble, and the system is solved using a Monte Carlo (MC) method. In such simulations, a given configuration evolves toward equilibrium as a Markov process, in which many small transitions in molecular configuration occur sequentially [15–18]. The transitions are implemented by probing an exchange of elements in the system; the exchange is accepted with a probability determined by the change in energy for that given exchange. Transitions that reduce the system energy are accepted with probability 1, while transitions that increase the energy by $\Delta E > 0$ are accepted with probability $\Pi = \exp(-\beta \Delta E)$. As the system evolves, the energetic characteristics of the interactions of the constitutive elements naturally determine the binding rates calculated from the flux between the states at that instant.

III. RESULTS AND DISCUSSIONS

We initialize the system consisting of F-actin, with its associated proteins Tm, Tn, Ca^{2+}, and S1 diluted in solutions with concentrations of C_F, C_{Tm}, C_{Tn}, $C_{Ca^{2+}}$, and C_{S1}, respectively. The actin concentrations C_F represent the concentration of actin monomers assembled in the actin filaments. The concentration of tropomyosin molecules in solution is sufficient to fully saturate the actin filaments, forming two continuous flexible chains (strands) along each actin filament. If present, Tn concentration in solution is sufficient to assemble TmTn complexes consisting of one Tn molecule and one Tm molecule interacting with seven actin monomers with stoichiometric ratios Tm:Tn:A of 1:1:7.

We first let F-actin, Tm, Tn, and Ca^{2+} reach equilibrium (50 Monte Carlo steps), then we add S1. At each Monte Carlo step, the algorithm visits all active elements that are bound with probability 1 and the active elements that are in solution with probability proportional to their concentrations. Then we test if each of these elements will change their current state. The solution concentrations of $C_{Ca^{2+}}$ and C_{S1} are defined as a fraction of elements in solution that will be visited at given instant. By mass conservation, if an active element unbinds, it will increase its respective free concen-

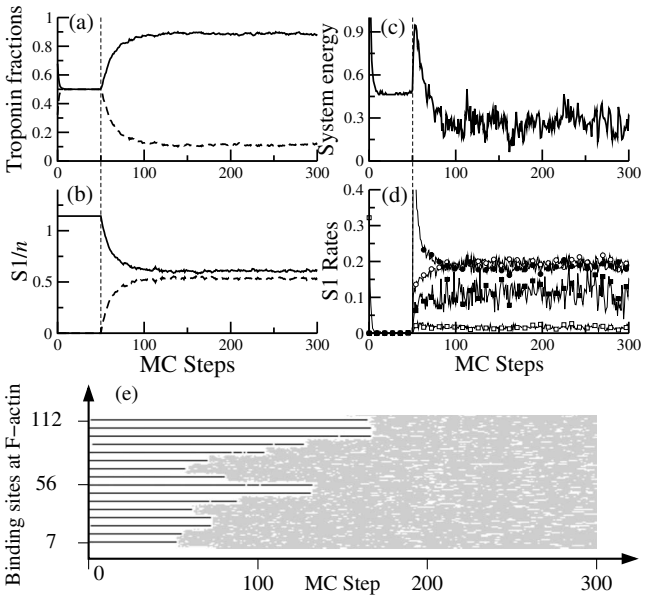

FIG. 3. Dynamics of TnI and myosin S1 binding to F-actin. In this simulation myosin is only added to the system after 50 MC steps. (a) Normalized free (line) and bound (dashed) TnI to F-actin; (b) ratio of free (line) and bound (dashed) S1 molecules to the total number of F-actin monomers; (c) the energy of the system (arbitrary units); (d) binding (open symbols) and unbinding (filled symbols) rates of myosin S1 (circle) and troponin Tn (square); (e) the simulated evolution in Monte Carlo steps of the chain of monomers of one F-actin. The configuration of the fiber at each MC step is represented by different pixel colors: white pixels represent empty sites, black pixels represent sites in which Tm is bound by a Tn forming a Tm·Tn complex, and gray pixels represent sites occupied by S1.

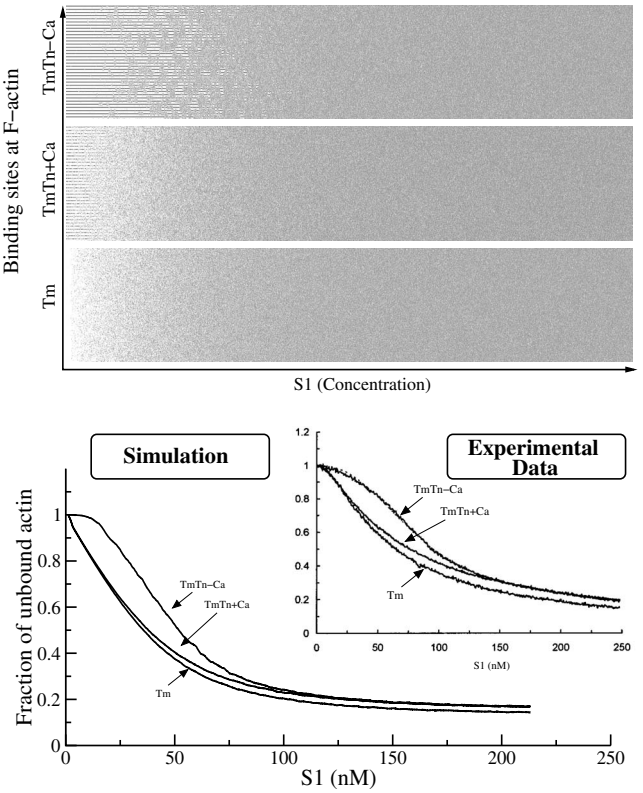

FIG. 4. Titration of actin filaments with S1 in the presence of either Tm or Tm·Tn simulated by the model. We used 5000 MC steps for a ramp increase in number of S1 molecules from 0 to 15000 and actin fiber with total of 3500 monomers (i.e., actin binding sites). Parameters used for this simulation are $\kappa=8.5\times10^{-44}$ Nm^4, $\alpha=0.13\times10^{-12}$ J/m, $\phi^{\Uparrow}=0.3$, $\phi^{\Downarrow}=-0.3$ rad, $E^{\Uparrow}=-0.3\times10^{-20}$ J, $E^{\Downarrow}=-1.2\times10^{-20}$ J $(-0.3\times10^{-20}$ J with $Ca^{2+})$, reference energy level of $E^{\varnothing}$ taken as zero. Top panel: graphical view representing the dynamics of S1 (gray), Tm·Tn complex (black), and empty sites (white). Bottom graph: fractions of unbound Tm for each case; the inset shows experimental results from Maytum *et al.* [19].

tration in solution. On the other hand, if a free active element binds a site it will decrease its concentration in solution.

Figure 3 shows the dynamics of the system evolving toward equilibration. In the first 50 Monte Carlo steps, there is no S1 in the system and the fraction of TnI attached to F-actin reaches equilibrium quickly and the fraction remains constant afterward [see Fig. 3(a)]. Similarly, the fraction of bound S1 molecules to actin sites also equilibrates within less than 100 MC steps [see Fig. 3(b)]; the total energy of the system is calculated from Eq. (8) and rapidly reaches a steady state [Fig. 3(c)]. Initially, the ratio of S1 molecules to the number of F-actin monomers is larger than 1 [Fig. 3(b)], meaning that there are more S1 molecules available than F-actin binding sites. Immediately after allowing S1 to bind, a spike in energy is observed [Fig. 3(c)] and within less than 100 MC steps the system reaches a new equilibrium, where only thermal fluctuations are observed. The state transition rates are determined by dividing the number of elements that move from one state to another within one MC step by the number of elements present at the original state. In Fig. 3(d) we show the rates of binding and unbinding at each MC step. These rates are commonly obtained from the best fits of the experimental data which requires multiple calculations of these rates. Here we demonstrate how they can be calculated. Finally, in Fig. 3 we show an example of the occupancy of all actin sites of an F-actin filament, by either S1 or TnI, evolving toward equilibration. Importantly, we notice that binding cooperativity naturally emerges from our model.

In Fig. 4, we validate our model by reproducing a common titration experiment from Maytum *et al.* [19]. The similarity between our model predictions and the experimental data is good, and strongly suggests that the cooperativity of binding leads to long-range correlation transmitted by the flexible Tm chain. Importantly, this is not a long-range interaction, but is a cooperative phenomenon as a result of the coupled contributions of nearest-neighbor interactions. One of the problems today in contractile biological system is to understand how this regulation works and our model offers an interpretation of this regulation based on a simple model of free-energy minimization. Regarding the agreement between our model and experimental data shown in Fig. 4, we feel that this similarity is an important confirmation that our model has captured the fundamental and essential physics of long-range cooperativity; we recognize that there remain deviations between the model predictions and experimental data, but suggest that these discrepancies are likely due to

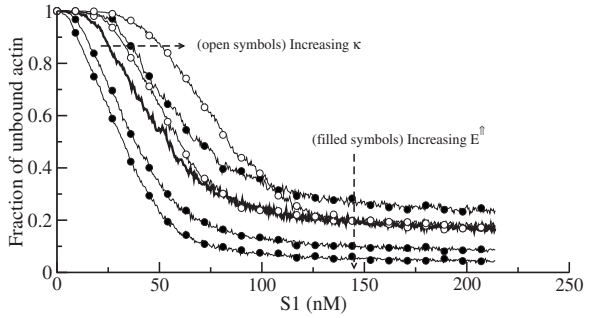

FIG. 5. Sensitivity analysis of titration of actin filaments with S1 in the presence of Tm·Tn simulated by the model. The thick solid black line is the reference curve, same as in Fig. 4. The lines with filled circles correspond to changing $E^{\Uparrow}$ from -0.20×10^{-20} J to -0.60×10^{-20} J in regular steps. The lines with open circles correspond to κ values of 8.5×10^{-44} Nm^4, 16.5×10^{-44} Nm^4, and 24.5×10^{-44} Nm^4.

higher order effects which remain as open questions.

Finally in Fig. 5 we show the sensitivity of the model predictions to variation in bending stiffness κ and the self-energy $E^{\Uparrow}$ of the S1 bound in spin-up state. Increase in κ delays cooperative binding of S1 to larger times, while increase in $E^{\Uparrow}$ speeds up binding of S1 at early times and the system reaches steady state much faster. These data clearly demonstrate the flexibility of the model to fit a variety of experimental data and predict rate constants.

The present work focuses on the regulation of myosin binding, without consideration of the initial assembly dynamics of a tropomyosin chain on actin and formation of (flexible) tropomyosin-troponin chain. The initial configuration in our system assumes that the tropomyosin-troponin chain is fully assembled and that all binding sites of actin surface are blocked by tropomyosin. In contrast, Vilfan [20] developed a theoretical model of rodlike tropomyosin binding to actin and assembly of a tropomyosin chain on actin, distinct from the regulation of myosin binding by tropomyosin. In future studies it will be interesting to consider both processes: that of tropomyosin binding on actin and assembly of the tropomyosin chain, coupled with the process of regulated myosin binding.

In summary, this Ising-like model incorporates the Tm chain bending stiffness which generates long-range correlation and cooperativity. We found that binding cooperativity emerges from the short-range nearest-neighbor interactions and the bending stiffness of the Tm chain.

ACKNOWLEDGMENTS

This work was supported by National Institute of Health Grant No. NIH R01 AR048776, Fundação de Amparo a Pesquisa do Estado de São Paulo (FAPESP) Grant No. 2006/06996-7, and LIM05 of HC-FMUSP. We thank Dr. D. A. Smith for helpful comments based on a careful reading of the paper.

[1] S. M. Gagne, S. Tsuda, M. X. Li, L. B. Smillie, and B. D. Sykes, Nat. Struct. Biol. **2**, 784 (1995).
[2] B. Tripet, J. E. van Eyk, and R. S. Hodges, J. Mol. Biol. **271**, 728 (1997).
[3] D. A. Smith and M. A. Geeves, Biophys. J. **84**, 3168 (2003).
[4] P. Vibert, R. Craig, and W. Lehman, J. Mol. Biol. **266**, 8 (1997).
[5] R. D. Bremel, J. M. Murray, and A. Weber, Cold Spring Harb. Symp. Quant. Biol. **37**, 267 (1973).
[6] L. E. Greene and E. Eisenberg, Proc. Natl. Acad. Sci. USA **77**, 2616 (1980).
[7] S. S. Lehrer and M. A. Geeves, J. Mol. Biol. **277**, 1081 (1998).
[8] A. M. Gordon, E. Homsher, and M. Regnier, Physiol. Rev. **80**, 853 (2000).
[9] J. C. Haselgrove, Cold Spring Harbor Symp. Quant. Biol. **37**, 341 (1973).
[10] H. E. Huxley, Cold Spring Harbor Symp. Quant. Biol. **37**, 361 (1973).
[11] D. A. Smith, R. Maytum, and M. A. Geeves, Biophys. J. **84**, 3155 (2003).
[12] Y. Chen, B. Yan, J. M. Chalovich, and B. Brenner, Biophys. J. **80**, 2338 (2001).
[13] D. A. Smith, J. Phys. A **34**, 4507 (2001).
[14] J. G. N. Phillips, J. P. Fillers, and C. Cohen, J. Mol. Biol. **192**, 111 (1986).
[15] K. Binder and D. W. Heermann, *Monte Carlo Simulation in Statistical Physics, an Introduction* (Springer, Berlin, Germany, 1997).
[16] A. M. Alencar, E. Wolfe, and S. V. Buldyrev, Phys. Rev. E **74**, 026311 (2006).
[17] N. Rosenblatt, A. M. Alencar, A. Majumdar, B. Suki, and D. Stamenovic, Phys. Rev. Lett. **97**, 168101 (2006).
[18] A. Majumdar, B. Suki, N. Rosenblatt, A. M. Alencar, and D. Stamenovic, Phys. Rev. E **78**, 041922 (2008).
[19] R. Maytum, S. S. Lehrer, and M. A. Geeves, Biochemistry **38**, 1102 (1999).
[20] A. Vilfan, Biophys. J. **81**, 3146 (2001).